Ecosystems
https://doi.org/10.1007/s10021-023-00871-z

Integrating Remote Sensing with Ground-based Observations to Quantify the Effects of an Extreme Freeze Event on Black Mangroves (*Avicennia germinans*) at the Landscape Scale

Melinda Martinez,[1]* Michael J. Osland,[1] James B. Grace,[1] Nicholas M. Enwright,[1] Camille L. Stagg,[1] Simen Kaalstad,[2] Gordon H. Anderson,[3] Anna R. Armitage,[4] Just Cebrian,[5,6] Karen L. Cummins,[7] Richard H. Day,[1] Donna J. Devlin,[2] Kenneth H. Dunton,[8] Laura C. Feher,[1] Alejandro Fierro-Cabo,[9] Elena A. Flores,[9] Andrew S. From,[1] A. Randall Hughes,[10] David A. Kaplan,[11] Amy K. Langston,[12] Christopher Miller,[13] Charles E. Proffitt,[2] Nathan G. F. Reaver,[11] Colt R. Sanspree,[14] Caitlin M. Snyder,[15] Andrew P. Stetter,[16] Kathleen M. Swanson,[17] Jamie E. Thompson,[3] and Carlos Zamora-Tovar[18]

[1]U.S. Geological Survey, Wetland and Aquatic Research Center, Lafayette, Louisiana, USA; [2]Texas A&M University—Corpus Christi, Corpus Christi, Texas, USA; [3]U.S. Geological Survey, Wetland and Aquatic Research Center, Gainesville, Florida, USA; [4]Texas A&M University at Galveston, Galveston, Texas, USA; [5]Northern Gulf Institute, Mississippi State University, Stennis Space Center, Mississippi, USA; [6]Vesta, PBC, San Francisco, California, USA; [7]Tall Timber Research Station, Tallahassee, Florida, USA; [8]Marine Science Institute, The University of Texas at Austin, Austin, Texas, USA; [9]University of Texas Rio Grande Valley, Brownsville, Texas, USA; [10]Northeastern University, Nahant, Massachusetts, USA; [11]University of Florida, Gainesville, Florida, USA; [12]Desert Research Institute, Reno, Nevada, USA; [13]Saint Leo University, St. Leo, Florida, USA; [14]U.S. Fish and Wildlife Service, Aransas National Wildlife Refuge, Austwell, Texas, USA; [15]Apalachicola National Estuarine Research Reserve, Eastpoint, Florida, USA; [16]U.S. Fish and Wildlife Service, Big Stone National Wildlife Refuge, Odessa, Minnesota, USA; [17]Mission-Aransas National Estuarine Research Reserve, Port Aransas, Texas, USA; [18]Universidad Autónoma de Tamaulipas, Ciudad Victoria, Tamaulipas, Mexico

Received 27 December 2022; accepted 21 July 2023

Supplementary Information: The online version contains supplementary material available at https://doi.org/10.1007/s10021-023-00871-z.

Author's contribution: MM, MJO, JBG, NME, and CLS conceived and designed the study. MM processed imagery, analyzed data, and created figures and tables with input from MJO, JBG, NME, and CLS. MM and MJO wrote the first full manuscript draft with input from JBG, NME, and CLS. SK, GHA, ARA, JC, KLC, RHD, DJD, KHD, LCF, AFC, EAF, ASF, ARH, DAK, AKL, BM, CM, MJO, CEP, NGFR, CRS, CMS, APS, KS, JET, CZT contributed ground-based mangrove damage data, which were organized by SK with input from data contributors. LCF created the data release of the ground-based data. All authors contributed to subsequent manuscript drafts and gave final approval.

**Corresponding author; e-mail:* melindmartinez@gmail.com

Published online: 14 August 2023

Abstract

Climate change is altering the frequency and intensity of extreme weather events. Quantifying ecosystem responses to extreme events at the landscape scale is critical for understanding and responding to climate-driven change but is constrained by limited data availability. Here, we integrated remote sensing with ground-based observations to quantify landscape-scale vegetation damage from an extreme climatic event. We used ground- and satellite-based black mangrove (*Avicennia germinans*) leaf damage data from the northern Gulf of Mexico (USA and Mexico) to examine the effects of an extreme freeze in a region where black mangroves are expanding their range. The February 2021 event produced coastal temperatures as low as − 10 °C in some areas, exceeding thresholds for *A. germinans* damage and mortality. We used Sentinel-2 surface reflectance data to assess vegetation greenness before and after the freeze, along with ground-based observations of *A. germinans* leaf damage. Our results show a negative, nonlinear threshold relationship between *A. germinans* leaf damage and minimum temperature, with a temperature threshold for leaf damage near − 6 °C. Satellite-based analyses indicate that, at the landscape scale, damage was particularly severe along the central Texas coast, where the freeze event affected > 2000 ha of *A. germinans*-dominated coastal wetlands. Our analyses highlight the value of pairing remotely sensed data with regional, ground-based observations for quantifying and extrapolating the effects of extreme freeze events on mangroves and other tropical, cold-sensitive plants. The results also demonstrate how extreme freeze events govern the expansion and contraction of mangroves near northern range limits in North America.

Key words: extreme freeze; mangroves; *Avicennia germinans*; sentinel-2; remote sensing; range limit; range expansion; ecological threshold; Gulf of Mexico.

Introduction

In the face of accelerating climate change (USGCRP 2017; IPCC 2021), ecologists are increasingly challenged to advance understanding of the ecological effects of changes in the frequency and intensity of extreme climatic events (Jentsch and others 2007; Smith 2011; USGCRP 2018). There is a particularly pressing need to better understand the effects of climate extremes that drive landscape-level shifts in dominant species via damage and mass mortality (Alber and others 2008; Allen and others 2010; Sippo and others 2018). Here, we coupled ground-based and remotely sensed measurements to examine the effects of an extreme winter storm that triggered landscape-scale damage to cold-sensitive coastal wetland vegetation near the transition between tropical and temperate ecosystems in North America.

In North America, the northern range limits of many tropical cold-sensitive organisms are governed by the frequency and intensity of extreme cold winter temperatures (Shreve 1914; Boucek and others 2016; Osland and others 2021; Walters and McClenachan 2021). Extreme cold events leading to mass mortality can result in range contraction (Lonard and Judd 1991; Martin and McEachron 1996; Stevens and others 2006). In contrast, consecutive winters without extreme cold events can lead to poleward range expansion (Purtlebaugh and others 2020; McClenachan and others 2021; Hesterberg and others 2022) and the tropicalization of temperate ecosystems (Osland and others 2021). The ecological influence of winter extremes is especially apparent within coastal wetlands, where extreme freezing and chilling temperatures greatly influence whether a coastal wetland is dominated by herbaceous or woody plants (Gabler and others 2017; Osland and others 2017; Cavanaugh and others 2019). While herbaceous salt marsh plants can tolerate extreme freeze events (Pennings and Bertness 2001), mangroves are tropical to subtropical, cold-sensitive woody plants that can be damaged or killed by extreme freeze events (Lugo and Patterson-Zuca 1977; Ross and others 2009; Lovelock and others 2016; Chen and others 2017). Thus, mangrove forests typically dominate tidal saline wetlands in warmer, tropical climates, and salt marshes typically dominate tidal saline wetlands in colder, temperate climates (Woodroffe and Grindrod 1991; Duke and others 1998). In the subtropics, there is a dynamic mix of salt marsh and mangroves, where dominance by either is dictated by preceding freeze event history (Gabler and others 2017; Osland and others 2017; Cavanaugh and others 2019).

Climate change is expected to produce warmer winters with declining frequency and intensity of winter cold temperature extremes (USGCRP 2017; IPCC 2021), which will enable the poleward range expansion of tropical, cold-sensitive species like mangroves. Mangrove expansion is of particular

importance for coastal ecosystems because it represents a state change from herbaceous marsh to coastal forest, impacting many ecosystem functions and services (Osland and others 2022). Mangrove range expansion, however, is not expected to occur in a continuous northward progression. Rather, occasional extreme freeze events near northern range limits are expected to produce landscape-scale damage and mortality, which means that range expansion is expected to be discontinuous and punctuated by freeze-induced range contraction events near poleward range limits (Boucek and others 2016; Langston and Kaplan 2020; Osland and others 2021).

Extreme freeze events leading to landscape-scale damage or mortality to mangroves near northern range limits have been understudied because they are unpredictable and infrequent. This is likely because of limited time or resources available for ecologists to rapidly redirect their attention to on-the-ground investigations of post-freeze ecological impacts (Jentsch and others 2007; Osland and others 2020). For example, the last major freeze event to result in mangrove mortality near range limits in Louisiana (USA) and Florida (USA) occurred in December 1989. While there are many mangrove mortality observations from that event documented in the literature (Stevens and others 2006; Osland and others 2017; McKee and Vervaeke 2018; Snyder and others 2022), there were no in-depth quantitative investigations of the landscape scale freeze impacts during the initial years following the event. However, recent computational advancements and improvements in remote sensing data provide enhanced opportunities for researchers to study landscape-scale damage and mass mortality.

The availability and spatiotemporal resolution of satellite-based data are improving rapidly, which means that remote sensing approaches are becoming increasingly valuable for quantifying landscape-scale vegetation damage from climate extremes. In particular, the Google Earth Engine platform has increased the accessibility of satellite images and provides the ability to quickly process thousands of images across space and time (Alonso and others 2016; Google Earth Engine 2022). Satellites such as Sentinel are particularly useful because of the higher spatial resolution (that is, 10-m compared to 30-m resolution via Landsat).

In February 2021, an extreme freeze event (Winter Storm Uri) resulted in landscape-scale damage to black mangroves (*Avicennia germinans*) in Texas (USA) along the northwestern Gulf of Mexico coast. In this study, we integrated remote sensing with regional, coordinated ground-based observations to investigate mangrove leaf damage during this event. More specifically, we investigated the following questions: (1) What regions experienced *A. germinans* leaf damage during the 2021 event and how severe was the damage; (2) Can we effectively assess mangrove leaf damage using satellite-based measurements before and after the freeze event; and (3) Are minimum temperature thresholds for leaf damage comparable between satellite-based data and ground-based data? To provide a historical perspective for this event, we also incorporated temperature records to determine how the 2021 freeze event compares with extreme winter temperatures that have occurred in Texas during the past eight decades (that is, 1942–2022).

Methods

Study Area and Study Design

Our study area included coastal wetlands along the northern Gulf of Mexico coast in northern Tamaulipas (Mexico; along the USA-Mexico border), Texas (USA), Louisiana (USA), and northern Florida (USA) (Figure 1). There are three common mangrove species in this region: the black mangrove (*A. germinans*), the red mangrove (*Rhizophora mangle*), and the white mangrove (*Laguncularia racemosa*). Our analyses focus on *A. germinans*, which is the most cold-tolerant of the three species and extends furthest north along the northern Gulf of Mexico coast (Sherrod and McMillan 1981, 1985; Pickens and Hester 2011; McKee and Vervaeke 2018; Snyder and others 2022). Hereafter, ''mangrove'' in the methods and results sections refers to *A. germinans*. In tropical regions, *A. germi-*

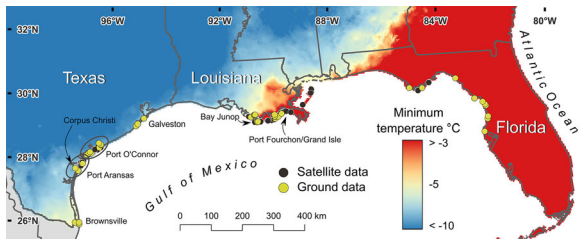

Figure 1. Location of the 375 data collection sites (circular symbols) along the northern Gulf of Mexico coast (USA), with minimum air temperatures during the February 2021 freeze event in the background. Our analyses incorporate data from 305 satellite sites and 70 ground observation sites. Minimum air temperatures were obtained from data produced by the Parameter-elevation Regressions on Independent Slopes Model (PRISM) climate group (prism.oregonstate.edu).

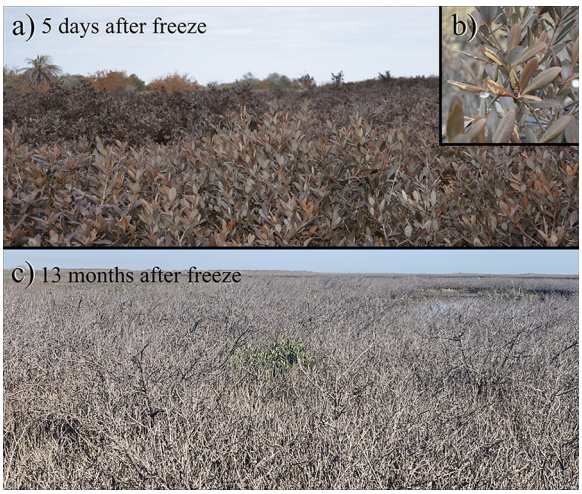

Figure 2. Photos of black mangrove (*Avicennia germinans*) damage in Port Aransas, Texas (USA) immediately after the 2021 freeze (**a** and **b**) and approximately 13 months later **c**. Photo credits: Ken Dunton (**a**, **b**) and Briana Martinez **c**.

nans individuals grow to become tall single-stemmed trees that form mangrove forests often greater than 10 m in height. However, near northern range limits along the northern Gulf of Mexico coast, *A. germinans* individuals are typically more shrublike, with multiple short stems often less than 2 m in height (Osland and others 2014; Yando and others 2016). Following cold events, *A. germinans* leaves can quickly turn brown and eventually fall from trees (Osland and others 2015, 2020; Feller and others 2022) (Figure 2). Leaves that are partially damaged during the initial days following a freeze event ultimately become fully damaged and are dropped from the trees. During moderate cold events (that is, temperatures between − 4 °C and − 7 °C), *A. germinans* individuals may lose leaves, branches, and/or stems (Osland and others 2015, 2020). However, *A. germinans* individuals are covered in regenerative buds that enable them to vigorously resprout and recover from moderate cold events (Lugo and Patterson-Zuca 1977; Tomlinson 2016). Full recovery from moderate events often occurs within the first several growing seasons (Osland and others 2015, 2020; Feller and others 2022). In some freeze events, *A. germinans* may lose all their aboveground biomass and resprout vigorously from the base. This basal resprouting is what produces the multi-stemmed shrublike morphology (Feller and others 2022). During severe cold events (for example, temperatures below − 7°), mangrove mortality can occur when belowground roots and basal regenerative buds are killed (Osland and others 2020).

We assessed mangrove damage and obtained temperature data from a total of 375 locations, which collectively represent a temperature and mangrove damage gradient (Figure 1) that we used to quantify temperature–damage relationships. Some of these locations were affected by the 2021 freeze event (Texas and parts of Louisiana), while other locations were unaffected by the freeze (Florida). Our analyses quantify mangrove leaf damage and temperature–damage relationships using two types of mangrove leaf damage data: satellite-derived data and ground-based data (that is, field-collected data). Satellite data were collected from 305 locations, and ground data were collected from 70 locations (Figure 1). Our analyses also incorporated two different types of minimum temperature data: historical station-based temperature data (that is, data for specific locations) and gridded temperature data (that is, raster data with continuous coverage across the study area).

Historical Station-Based Temperature Data (1942–2022)

Station-based data were used to provide a historical, long-term perspective (1942–2022) of extreme minimum temperatures. We obtained daily minimum temperature data (that is, the coldest temperature recorded each day) from the Global Historical Climatology Network (GHCN) database for Texas stations in Brownsville (station: USW00012919), Corpus Christi (station: USW00012924), and Galveston (stations: USW00012923, USC00414531 and USW00012944) (NOAA 2022), from which we incorporated data from 1946–2022 (Brownsville), 1942–2022 (Corpus Christi), and 1946–2022 (Galveston). We used a similar approach to Snyder and others (2022), where calendar years were converted to winter years (that is, November to March) to assign freeze events to winters (for example, the December 1989 freeze was assigned to the 1989 winter and the February 2021 freeze was assigned to the 2020 winter). Then, for each winter year, we determined the annual minimum temperature (that is, the absolute minimum daily temperature that occurred that winter year). Next, we identified winter years with minimum temperatures below literature-based temperature thresholds for *A. germinans* leaf damage and mortality (that is, − 4.2 °C and − 6.6 °C, respectively) (Osland and others 2020). These data were also

used to highlight recent consecutive years without freeze events leading to mangrove mortality.

Gridded Temperature Data—2021 Freeze Event

Gridded temperature data were used to determine the minimum temperatures for each of the 375 mangrove damage point locations. We determined the minimum temperatures that occurred during the 2021 freeze event using the location coordinates and 4-km resolution continuous, gridded daily minimum air temperature data produced by the PRISM (Parameter-elevation Regression on Independent Slopes Model) Climate Group at Oregon State University (prism.oregonstate.edu). These data were created using the PRISM interpolation method (Daly and others 2008). The PRISM model is valuable in this region because the data capture the influence of land–ocean temperature gradients (Daly and others 2003, 2008, 2012), which play an important ecological role during freeze events in the coastal zone (Osland and others 2017; Snyder and others 2022). Prior analyses have demonstrated a strong correlation between PRISM data and ground-based, logger-derived air temperature data (Osland and others 2020).

Ground-Based Mangrove Damage Data

After the 2021 freeze event, ground-based mangrove damage data were collected through collaborative contributions of researchers across the northern Gulf of Mexico (Figure 1), including locations in Florida (total ground locations: 14), Louisiana (total ground locations: 16), Texas (total ground locations: 27), and northern Tamaulipas (total ground locations: 3). The locations in Tamaulipas were close to the USA-Mexico border and incorporated into the Brownsville region. At each location, collaborators visually estimated the percentage (0–100%) of leaves showing freeze damage within 100-m^2 plots. These surveys were conducted between 25 February and 27 April of 2021. If a mangrove showed all brown leaves or had already lost all of leaves, leaf damage was recorded as 100%. These data have been published and are publicly available as a U.S. Geological Survey data release (Kaalstad and others 2023). At 10 sites, mangrove leaf damage was estimated at the 100-m^2 plot-level (that is, percentage of leaves showing freeze damage for all mangrove individuals within the 100-m^2 plot). At 60 of the sites, mangrove leaf damage was estimated for individual trees within a 100-m^2 plot (that is, 1–9 trees per plot), and the individual tree measurements were converted to plot-level means. For more details regarding the ground-based leaf damage measurements, see Kaalstad and others (2023).

Satellite-Based Mangrove Damage Data

Mangrove range limits are often difficult to delineate with remotely sensed data because their distribution shifts in response to changing environmental conditions. In the northern Gulf of Mexico, there is no region-wide dataset that adequately captures the distribution of mangroves near the northern range limits covered in this study, though efforts to fill this gap are underway (Bardou and others 2022, 2023). As an initial regional screening, we used a recently produced mangrove presence dataset (Bardou and others 2022). This dataset identifies mangrove presence within 1/8-degree cells (that is, resolution of approximately 14 km-by-16 km) (Figure 3a). To identify point locations for obtaining site-specific satellite data observations of mangrove damage (Figure 1), we compiled mangrove distribution data from several local datasets (Finkbeiner and others 2009; Osland and others 2017; Day and others 2020; Enwright and others 2020; Snyder and others 2022) (Table S1). For raster and polygon vector data, points were randomly created within mangrove areas and verified using recent Google Earth aerial imagery (Figure 3a). Data points that were near mangrove patch edges or in open water were excluded. All location datasets were merged, and points were randomly selected by region, producing a final dataset that included 305 total sites for satellite data collection. The number of satellite points varied by region as follows: Florida (total satellite locations: 30), Louisiana (total satellite locations: 100), and Texas (total satellite locations: 175). To further elucidate the effects of the 2021 freeze across the central Texas coast where damage was particularly severe, some of our analyses separate the data in Texas into the following two regions: Port Aransas (total satellite locations: 68), Port O'Connor (total satellite locations: 107) (Figure 1). There was limited satellite data within the Galveston region because mangrove coverage was too low due to the higher frequency and intensity of freeze events. The few *A. germinans* mangroves that can be found near the Galveston area are sparse and usually less than 1 m in height.

Sentinel-2 surface reflectance data (that is, atmospherically corrected data) were used to detect greenness changes in remotely sensed imagery.

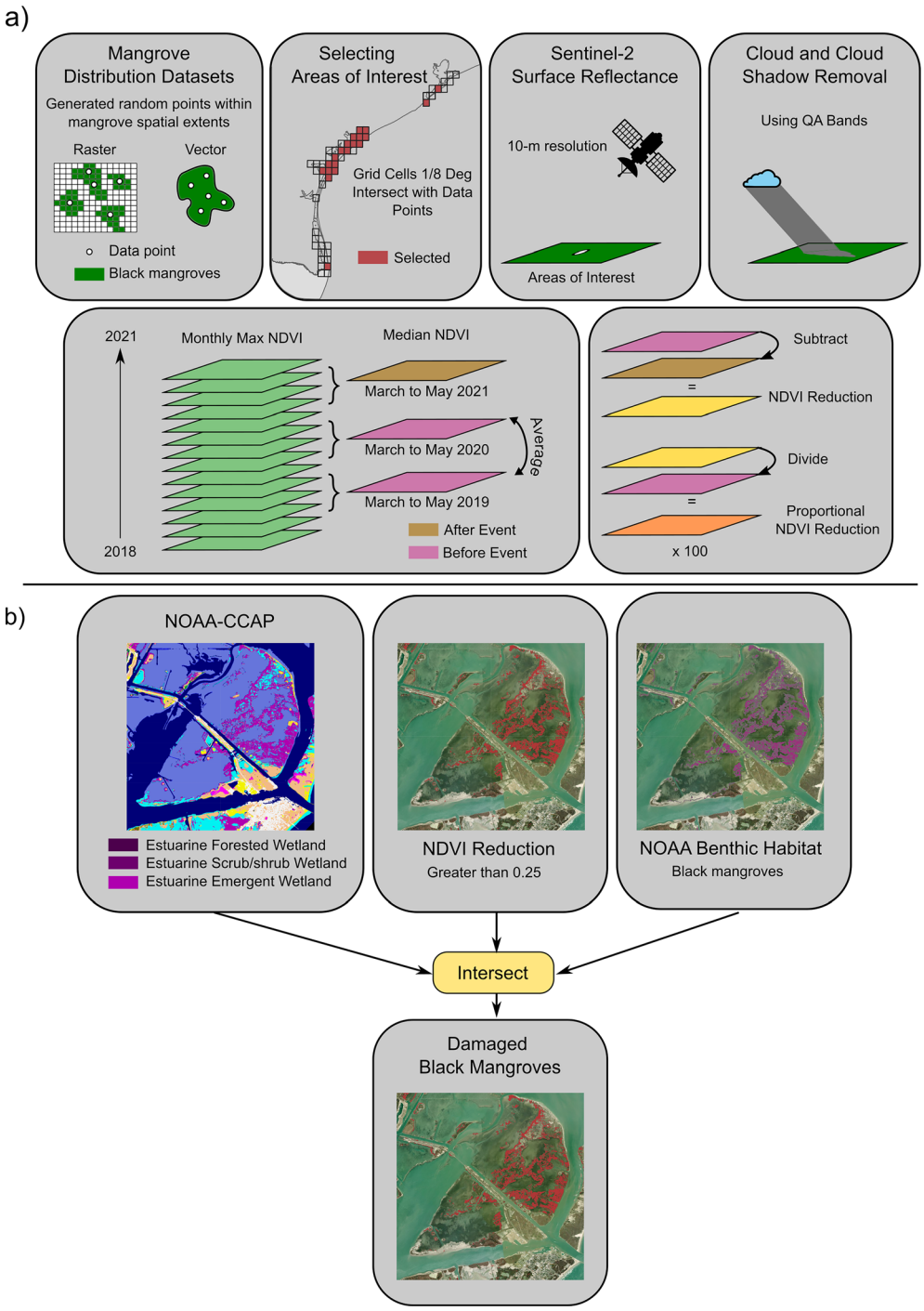
a)
Mangrove Distribution Datasets
Generated random points within mangrove spatial extents
Raster
Vector
Data point
Black mangroves
Selecting Areas of Interest
Grid Cells 1/8 Deg Intersect with Data Points
Selected
Sentinel-2 Surface Reflectance
10-m resolution
Areas of Interest
Cloud and Cloud Shadow Removal
Using QA Bands
2021
2018
Monthly Max NDVI
Median NDVI
March to May 2021
March to May 2020
March to May 2019
Average
After Event
Before Event
Subtract
=
NDVI Reduction
Divide
=
Proportional NDVI Reduction
x 100
b)
NOAA-CCAP
Estuarine Forested Wetland
Estuarine Scrub/shrub Wetland
Estuarine Emergent Wetland
NDVI Reduction
Greater than 0.25
NOAA Benthic Habitat
Black mangroves
Intersect
Damaged Black Mangroves

◀**Figure 3.** Geospatial methods for **a** selecting mangrove sites and processing satellite imagery using mangrove distribution datasets and **b** quantifying the spatial extent of mangrove damage. Before processing satellite images, we compiled mangrove distribution datasets, which were in the form of either classified vector or raster data. Random data points within vector or raster data were created and used as satellite-based sites for data extraction. To reduce spatial image processing to a defined area of interest, the newly created data points were intersected with grid cell vector data of known mangrove locations based on expert knowledge (Bardou and others 2022). Sentinel-2 surface reflectance image data were then restricted to the areas of interest. Images were processed to remove clouds and cloud shadows. Monthly max (per pixel) Normalized Difference Vegetation Index (NDVI) composites were generated from December 2018 to December 2021. Then the median NDVIs from March to May for each year (2019, 2020, and 2021) were calculated per pixel. The years 2019 and 2020 were averaged together and classified as 'Before' the freeze event, while 2021 was classified as 'After' the freeze event. The difference between NDVI values before and after was used as the total NDVI reduction. Proportional NDVI was calculated by dividing the NDVI reduction by the NDVI values before the event and then multiplied by 100. The geospatial methods for quantifying the spatial extent of mangrove damage used included: (1) identifying mangrove areas using land cover data from National Oceanic and Atmospheric Administration (NOAA) Coastal Change Analysis Program (C-CAP), benthic habitat data from NOAA, and the NDVI reduction data. For the NDVI reduction data, we only included areas where NDVI decreases were greater than 0.25. The spatial extents where all three datasets intersected were used to produce a final mangrove damage spatial extent. Note that mangrove damage spatial extent was quantified for central Texas coast only.

Data were acquired for each of the 305 locations using Google Earth Engine, a cloud-based platform (Google Earth Engine, 2022) (Figure 3a). Sentinel-2 has a revisit time of approximately six days and a resolution of 10-m. Monthly, cloud-free composites were generated using the maximum Normalized Difference Vegetation Index (NDVI) for the period from December 2018 to December 2021. We used the cloud probability mask band (MSK_CLDPRB) to remove pixels with cloud probability greater than 5%, as well as the scene classification band (SCL) to remove cloud shadows and cirrus clouds (that is, bit value 3 and 10, respectively). NDVI uses the red (RED) and near-infrared (NIR) bands as follows: (NIR-RED)/(NIR + RED) (Rouse and others 1974). Pixel-maximum NDVI was chosen over median NDVI to reduce potential for measurement errors from clouds and haze, as well as low NDVI from tidal flooding. Monthly NDVI time series were extracted from satellite data for the 305 satellite locations. Unfortunately, images for mangroves within the Brownsville, TX area were limited because of lack of cloud-free Sentinel-2 data for that area during the months of March to May 2021, which is the post-freeze period that is critical for assessing freeze damage.

Mangrove damage from satellite data was calculated in two ways: NDVI reduction and proportional NDVI reduction. We used the median of the maximum NDVI monthly composites from the same period (March to May) before and after the event for both approaches (Figure 3a). The same periods were used each year to minimize seasonality effects. The before event period ($NDVI_{Before}$) incorporated two years of data before the event (that is, March to May for years 2019 and 2020). The after-event period ($NDVI_{After}$) incorporated data from three months immediately after the freeze (that is, March to May of 2021). NDVI reduction was calculated as the difference between $NDVI_{Before}$ and $NDVI_{After}$. The proportional NDVI reduction was calculated as the difference between $NDVI_{Before}$ and $NDVI_{After}$ divided by $NDVI_{Before}$, multiplied by 100. For NDVI reduction, values less than zero are possible for pixels where $NDVI_{After}$ was slightly higher than $NDVI_{Before}$ in unaffected areas. Thus, for the proportional NDVI reduction calculations, the minimum value possible was set to zero and maximum value set to 100.

Data Analyses: Temperature Thresholds

We used nonlinear logistic regression analyses to quantify the relationships between minimum temperature and mangrove damage. Curves were developed separately using ground-based data and satellite-based data. To identify minimum temperature thresholds for mangrove damage, we used the first and second derivatives of the logistic models to determine: (1) the inflection point that represents the location of maximum rate of change (T) and is the local maxima of the first derivative of the logistic model, and (2) the maximum rate of change that was determined as the area between local maxima and minima peaks of the second derivative of the logistic model, whereas T represents a discrete threshold and the absolute location of the highest rate of change in mangrove damage, and the area of maximum rate of change represents a threshold range where the rate of change is

highest. For more information regarding the use of area of maximum rate of change and inflection points to detect thresholds, see Wilson and Agnew (1992), Timoney and others (1993), Hufkens and others (2008), and Frazier and Wang (2013). All data analyses were performed in R (R Core Team 2022). Logistic regression analyses were conducted using the *drc* package (Ritz and Strebig 2016).

Data Analyses: Ground-Based vs Satellite-Based Mangrove Damage

To compare our ground-based mangrove damage measurements with the satellite-based mangrove damage measurements, we identified a subset of 36 sites where we could obtain both kinds of data. To be included in this analysis, mangrove coverage had to be extensive enough to cover the corresponding 10-m satellite pixel, which was determined using Google Earth imagery. We extracted satellite data for these 36 ground-based data points and determined the NDVI reduction using the two calculations described previously. Logistic regression analyses were used to quantify the relationships between ground-based and satellite-based mangrove damage data.

Landscape-Scale Mangrove Damage (central Texas Coast Only)

One of our goals was to test whether NDVI reduction calculations could be used to characterize mangrove damage across the landscape. Within the 1/8-degree grid cells covering an area of 10,752 km^2, we applied the two NDVI reduction calculations per pixel (Figure S1). Grid cells in Texas cover an area of 4,480 km^2, in Louisiana an area of 5,376 km^2, and in Florida an area of 896 km^2. To illustrate the mangrove damage following the 2021 freeze event for central Texas coast only, we isolated mangrove spatial extents from several layers and compiled them into a single layer (Figure 3b). We acquired coastal wetland coverage data from the National Oceanic and Atmospheric Administration (NOAA) 2015–2017 Coastal Change Analysis Program-Beta (C-CAP) 10-m resolution land cover dataset (Office for Coastal Management 2022) (Figure 3b). To identify vegetated coastal wetlands, we incorporated the following C-CAP classes: estuarine forested wetland, estuarine scrub/shrub wetland, and estuarine emergent wetland. Although these data do not explicitly delineate mangroves, they do identify areas that are coastal wetlands. We also selected all areas identified as mangroves in a benthic habitat map produced by Finkbeiner and others (2009) (Figure 3b). The two datasets were merged to create a single mangrove habitat map for analysis. Our NDVI reduction metrics were then used to identify coastal wetland areas where mangrove damage occurred (Figure 3b).

Results

Historical Station-Based Temperature Data (1942–2022)

The station-based temperature data show that the Galveston area has had 11 consecutive years of winters without a freeze event, and more frequent and recent freeze events cold enough to cause *A. germinans* damage and/or mortality than other regions in the study area (see points in 1989, 2000, 2010, and 2018 that fall below or near horizontal dashed threshold lines in Figure 4). In contrast, before the 2021 freeze event, the Corpus Christi and Brownsville regions had 31 consecutive winters without a freeze event below the threshold for *A. germinans* mortality (note the absence of points below the mortality threshold line during 1989–2021 in Figure 4). The last major mangrove-relevant freeze event for Corpus Christi and Brownsville occurred in 1989. Of the three regions, Brownsville is the warmest area with the fewest freeze events during the last eight decades that could have led to *A. germinans* damage or mortality. The December 1989 event was the last major freeze event to affect all three regions (that is, Galveston, Corpus Christi, and Brownsville) with temperatures cold enough to cause *A. germinans* mortality (Figure 4a–c). The station-based temperature data indicate that freeze events in January 1947, January 1951, January 1962, and December 1983 were also cold enough to affect *A. germinans* in all three regions.

Temperatures During the 2021 Freeze Event (Gridded PRISM Data)

During the 2021 freeze event, recorded temperatures cold enough to cause mangrove damage (that is, less than − 4 °C) occurred between 15 and 17 February, 2021. The Port Aransas and Galveston regions both had minimum temperatures near − 8 °C. Minimum temperatures in the coastal region near Brownsville were as low as − 5 °C. Western coastal Louisiana also experienced minimum temperatures near − 5 °C. The coldest temperatures experienced along the northern Florida coast during this event were near 2.5 °C.

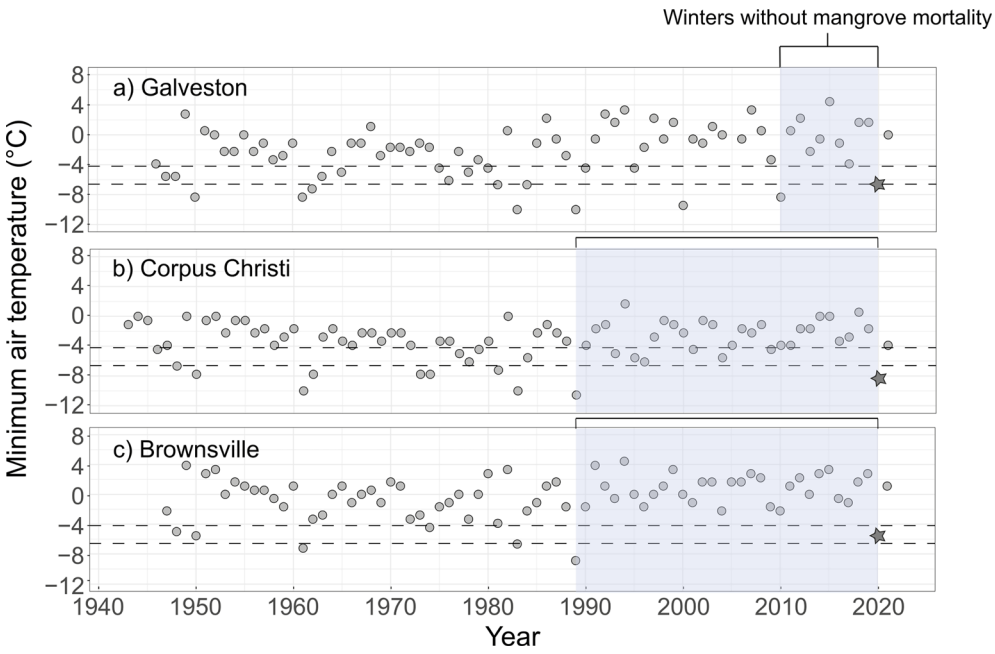

Figure 4. Annual winter minimum air temperatures for Galveston **a**, Corpus Christi **b**, and Brownsville **c**, Texas (USA) for the 79-year period extending from 1942 to 2021. Stars denote the minimum temperature during the February 2021 freeze event. Horizontal dashed lines are literature-based temperature thresholds for black mangrove (*Avicennia germinans*) leaf damage and mortality (that is, − 4.2 °C and − 6.6 °C, respectively) (Osland and others 2020). Events below these lines are expected to have caused leaf damage or mortality, respectively. The translucent purple areas within panels highlight recent consecutive years without freeze events potentially leading to mangrove mortality.

Satellite-Based Mangrove Damage

The browning of mangrove leaves (Figure 2), which was reflected in satellite images (Figure 5), occurred shortly after the freeze event. The NDVI time series by region showed clear and rapid declines in NDVI after the freeze event in the Port Aransas and Port O'Connor regions (Figure 5), although there was some variability by region (Figure S2). For Port Aransas and Port O'Connor, mangrove NDVI before the freeze event (March to May 2019 and 2020) was five times higher than after the freeze (March to May 2021) (Table 1). There were no changes in NDVI for the Louisiana and Florida regions (Table 1). There was considerable spatial variation in the severity of satellite-based mangrove damage within the Port Aransas and Port O'Connor regions (Figure 6b and c; see vertical spread of points for these two regions), compared to ground data. Sites with minimum temperatures less than − 7.5 °C had an NDVI reduction ranging from − 0.17 to − 0.72 (Figure 6b), equivalent to a proportional NDVI reduction from 28 to 100% (Figure 6c). There was a strong nonlinear relationship between satellite-based and ground-based mangrove damage (Figure S3). Threshold analyses indicate that ground-based mangrove damage values near 100% are likely when NDVI reduction values are less than 0.05 and proportional NDVI reduction values are greater than 12% (Figure S3). The magnitude of satellite-based NDVI reduction was highly variable for areas where ground-based leaf damage was near 100% (Figure S3), which helps explain the large variation in NDVI reduction in Figure 6b and c.

Ground-Based Mangrove Damage

Avicennia germinans individuals in the mid to northern Texas coastal regions (that is, Galveston, Port O'Connor, and Port Aransas) experienced the greatest leaf damage from the 2021 freeze event (Figure 6a and see photos in Figure 2) (Kaalstad and others 2023). Mean ± sd ground-based leaf damage was 100 ± 0%, 100 ± 0%, and 97 ± 10% for Galveston, Port O'Connor, and Port Aransas, respectively. The leaf damage in the Brownsville region ranged from 0 to 69%. There was minor leaf damage in western Louisiana near Bay Junop, where leaf damage was below 50%, but no *A. germinans* freeze damage in eastern Louisiana near Port Fourchon and Grand Isle. There was no freeze

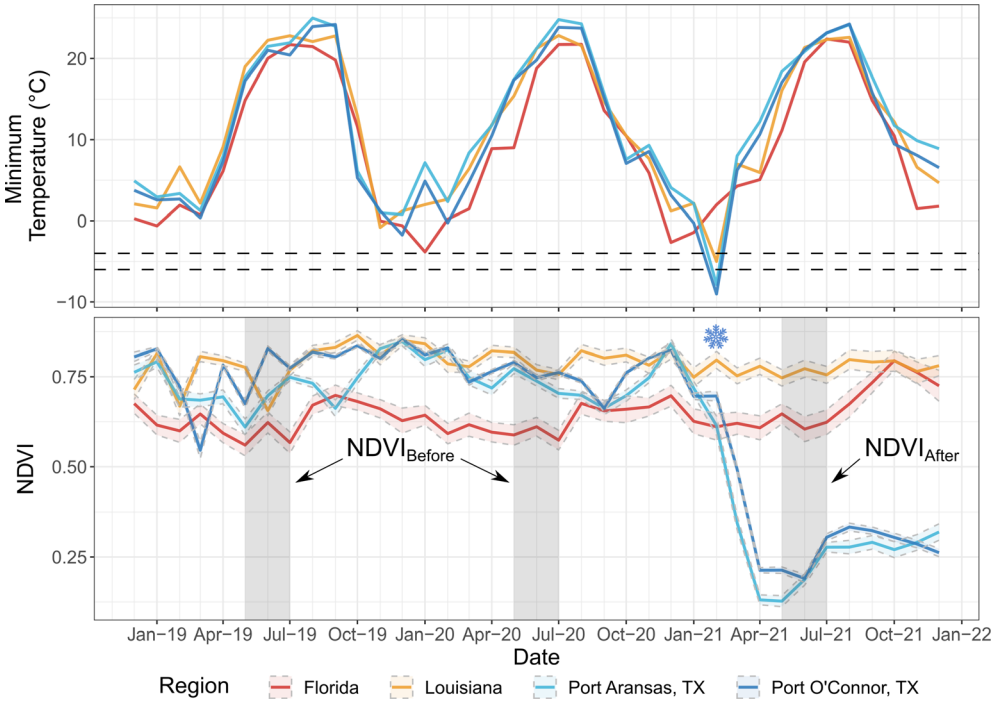

Figure 5. Monthly minimum temperature (°C) using PRISM data and mean (± SE) Normalized Difference Vegetation Index (NDVI) for black mangroves (*Avicennia germinans*) by region using the satellite data points from Figure 1. Horizontal dashed lines (top panel) are literature-based temperature thresholds for black mangrove (*Avicennia germinans*) leaf damage and mortality (that is, − 4.2 °C and −6.6 °C, respectively) (Osland and others 2020). The snowflake symbol (bottom panel) denotes the February 2021 freeze event. The vertical gray rectangles (bottom panel) represent months that were used for mangrove damage analyses, $NDVI_{Before}$ March to May 2019 and 2020 and $NDVI_{After}$ March to May 2021. NDVI is a commonly used vegetation index that can be used to quantify the greenness of a pixel area. We used changes in NDVI to quantify mangrove leaf damage or loss due to the 2021 freeze event (for example, see photos in Figure 2 and abrupt decrease in NDVI in Port Aransas and Port O'Connor following the event).

Table 1. Summary of Normalized Difference Vegetation Index (NDVI; Mean ± sd) by Region for Mangroves Before and After the 2021 Freeze Event

Region	$NDVI_{Before}$	$NDVI_{After}$
Florida	0.62 ± 0.15	0.62 ± 0.17
Louisiana	0.76 ± 0.12	0.76 ± 0.22
Port O'Connor, Texas	0.73 ± 0.11	0.31 ± 0.15
Port Aransas, Texas	0.70 ± 0.16	0.20 ± 0.17

Note the large decrease in NDVI in the Port O'Connor and Port Aransas regions.

damage to mangroves in Florida from the 2021 event.

Minimum Temperature Thresholds for A. Germinans Leaf Damage

Minimum temperature thresholds for *A. germinans* leaf damage based upon ground data and satellite data were near − 6.0 °C, although there is less certainty with satellite-based data because of the lack of data points near − 6.0 °C (Figure 6a–c). The minimum temperature threshold from ground data was determined to be − 5.7 °C (threshold range: − 6.3 °C to − 5.2 °C) (Figure 6a). For satellite-based data using the NDVI reduction metric, the threshold was determined to be − 6.4 °C (threshold range: − 6.7 °C to − 6.2 °C) (Figure 6b). For satellite-based data using the proportional NDVI reduction metric, the threshold was determined to be − 6.0 °C (threshold range: − 6.4 °C to − 5.7 °C) (Figure 6c). All nonlinear logistic regressions were significant ($p < 0.01$).

Landscape-Scale Mangrove Damage (Central Texas Coast Only)

Satellite data indicate that landscape-scale mangrove damage was particularly severe along the central Texas coast near Port O'Connor and Port Aransas (Figure 7a and b, respectively). Mangrove damage was slightly more severe in Port Aransas compared to Port O'Connor. The NDVI reduction

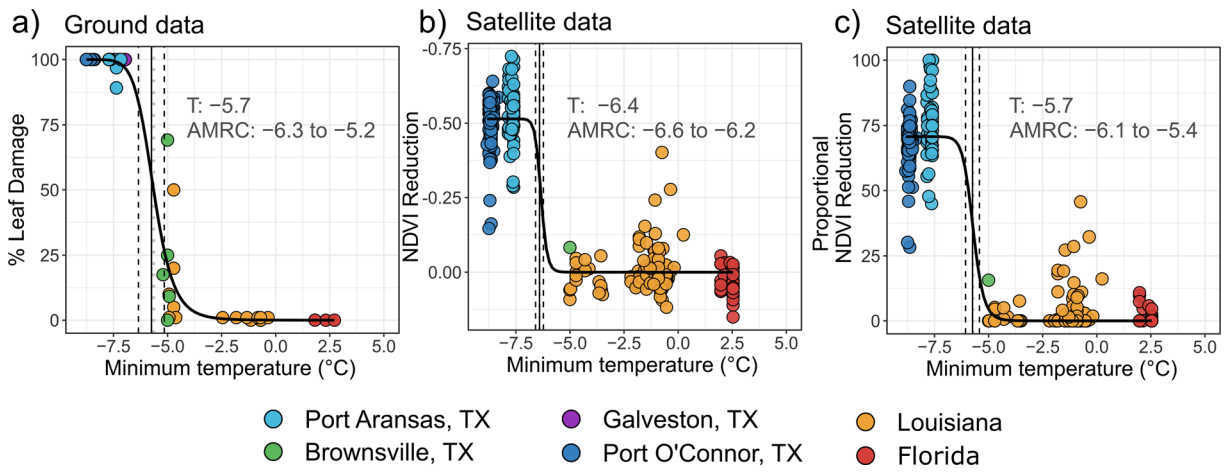

Figure 6. The nonlinear logistic relationships between minimum air temperature using PRISM data and black mangrove (*Avicennia germinans*) leaf damage as measured by **a** ground-based observations of leaf damage, **b** satellite-based Normalized Difference Vegetation Index (NDVI) reduction, and **c** satellite-based proportional NDVI reduction. Solid vertical lines within-panel indicate discrete minimum temperature thresholds (T), while vertical dashed lines indicate threshold ranges [that is, areas of maximum rate of change (AMRC)]. Note that data from Galveston and Brownsville sites are only in panel a (ground data); appropriate satellite data from those two areas were not available for inclusion in panels b and c.

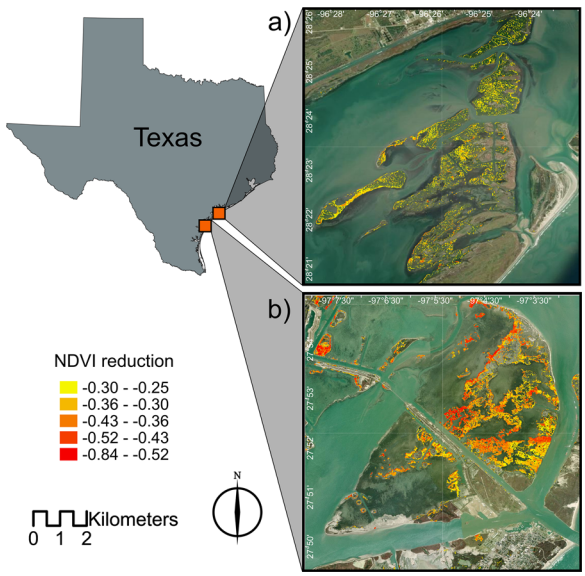

Figure 7. Landscape-scale mangrove damage was particularly severe along the central Texas coast near Port O'Connor **a** and Port Aransas **b**. For each location, mangrove damage is shown using mean Normalized Difference Vegetation index (NDVI) reduction (see Figure 5 for temporal window used). The scale and compass heading apply to both panels **a** and **b**.

approach indicates that mangrove damage in the Port Aransas and Port O'Connor regions occurred in at least 1,215 and 1,037 ha of coastal wetlands, respectively. The proportional NDVI reduction approach reflected a similar pattern of landscape-scale mangrove damage.

Discussion

Our results show that satellite imagery and NDVI metrics, in combination with mangrove and/or coastal wetland distribution data, can be used to investigate spatial and temporal patterns of mangrove leaf damage from freeze events, adding to previous studies demonstrating the utility of satellite-based measurements of mangrove vegetation change (Cavanaugh and others 2014, 2018; Zhang and others 2016; Lagomasino and others 2021). Our results also demonstrate the power of integrating remote sensing with regional, coordinated ground-based observations, which enabled us to investigate mangrove damage at larger spatial and temporal scales compared to field-based methods alone.

Despite the many benefits of remote sensing, there are some challenges and limitations of using satellite-based data to assess mangrove freeze damage. For example, satellite image resolution directly affects image processing time, which affects many steps including the removal of clouds and cloud shadows, the creation of monthly composites, and the development of pixel-based metrics (Tahsin and others 2018). Poor temporal resolution can also present a challenge, as there were some mangrove regions (for example, south Texas near Brownsville) that were not included in remote

sensing analyses because of cloud contamination. There are higher resolution satellites available, such as 3-m PlanetScope imagery, that can potentially detect smaller mangrove patches, but finer resolution involves longer processing times.

Geometric correction issues and the need for tight image co-registration can also present challenges when using finer resolution data, such as PlanetScope (Frazier and Hemingway 2021). If there were pixels with fewer observations, it is possible the maximum NDVI was artificially lower due to flooding. The spatial configuration of mangroves can also be a limitation, as mangroves are often found along wetland edges that may not completely cover a satellite image pixel (Wang and others 2019), which can lead to pixel purity issues (that is, having more cover types than just mangroves in a pixel). Pixels that have open water/water edge in them will have lower NDVI even without any vegetation differences among them. The mixed pixel issues may also explain the large amount of variation in NDVI reduction (Figure 6b and c) as well as the nonlinear relationship between ground-based and satellite-based methods (Figure S3). The variation in NDVI may also have been caused by mangrove phenology differences in the years prior to freeze, as phenology is known to respond to seasonal cycles in temperature, precipitation, and nutrients (Zhang and others 2016).

Our analyses quantify the landscape-scale damage to mangroves that occurred across the Texas coast during the 2021 freeze event, but our measurements do not quantify mangrove mortality or recovery. *Avicennia germinans* plants can rapidly resprout and recover from moderate freeze events that cause damage but do not lead to mortality (that is, freeze events with temperatures between − 4 °C and − 7 °C) (Osland and others 2020). However, temperatures less than − 7 °C can lead to mortality (Osland and others 2020) and an extended period of recovery (Stevens and others 2006; Cavanaugh and others 2019). Mangrove mortality and recovery during the 2021 event are currently unknown and warrant further investigation.

Future research is needed to investigate: (1) mangrove mortality during the 2021 freeze event; (2) mangrove recovery after the freeze event; (3) mangrove life stages that were most affected by the freeze (Pickens and Hester 2011; Coldren and Proffitt 2017; Macy and others 2021; Hoffman and others 2022); and (4) whether certain landscape positions helped mangroves survive the freeze event because of abiotic differences (Weaver and Armitage 2018; Feller and others 2022) or microclimatic conditions that provided a buffering effect against the freeze event (Ross and others 2009; Devaney and others 2017; Osland and others 2019). The utility of other vegetation and water indices, such as Normalized Difference Water/Moisture Index or Visible Atmospheric Resistant Index, should also be evaluated because NDVI can be sensitive to the presence of moist soils and water (Gao 1996; Gitelson and others 2002). Alternatively, pixels could be screened and filtered for tides with a tide index appropriate for moderate spatial resolution pixels, such as FLATS (Narron and others 2022).

Our analyses show that the minimum temperature thresholds for mangrove leaf damage quantified using satellite-based data are similar to thresholds determined from ground-based data. This finding opens the door to new investigations because satellite-based mangrove damage data and gridded temperature data are more widely available and span larger temporal and spatial scales than field-based measurements. During the 2021 event, the minimum temperature threshold for *A. germinans* leaf damage was determined to be near − 6 °C. During a 2018 freeze event, the minimum temperature threshold for *A. germinans* leaf damage was determined to be slightly warmer (that is, near − 4 °C) (Osland and others 2020).

There are many factors that could explain the differences in temperature threshold between these two studies, including freeze duration, the quality of temperature data (that is, local, ground-based data vs. gridded interpolated data from adjacent areas), microclimatic variation (Ross and others 2009; Devaney and others 2017; Osland and others 2019), conditions preceding the freeze event, nutrient enrichment (Feller and others 2022), and intraspecific and life-stage dependent differences in freeze tolerance (Pickens and Hester 2011; Coldren and Proffitt 2017; Macy and others 2021; Hoffman and others 2022). Collectively, these two studies indicate that within the northern Gulf of Mexico, *A. germinans* leaf damage is likely to occur when temperatures are below the following range: − 4 °C to − 6 °C. Temperature thresholds for *A. germinans* individuals in south Florida are expected to be higher due to the decreased exposure of *A. germinans* individuals to temperatures of this magnitude as well as natural selection processes that have resulted in adaptive genetic differentiation (Sherrod and McMillan 1985; Madrid and others 2014; Cook-Patton and others 2015; Kennedy and others 2020, 2022).

In this study, we demonstrate a multi-step process (Figure 3) for using satellite-based data in

combination with ground-based observations to expand the spatial and temporal extent over which mangrove damage and recovery can be quantified. As climate change continues to accelerate and satellite data continue to improve, the use of remote sensing technology will become increasingly valuable for assessing vegetation damage and recovery following extreme events. Collectively, our analyses show the value of integrating remotely sensed data with regional, coordinated ground-based freeze damage observations for quantifying the effects of extreme freeze events on mangroves and other tropical, cold-sensitive plants. In a rapidly warming world where tropical and subtropical species are increasingly moving poleward in response to changes in the frequency and intensity of extreme cold events, this information regarding freeze tolerances and sensitivities is needed to better anticipate and prepare for rapidly changing range limits.

ACKNOWLEDGEMENTS

We thank Kristin Byrd for helpful comments on an earlier version of the manuscript. MM was supported by a USGS Mendenhall Postdoctoral Research Fellowship funded by the USGS Ecosystems Mission Area and the USGS Wetland and Aquatic Research Center. This research was also partially supported by the USGS Climate Research and Development and the USGS Greater Everglades Priority Ecosystem Science programs. Any use of trade, firm or product names is for descriptive purposes only and does not imply endorsement by the US Government.

DATA AVAILABILITY

The data from this study are available within the following U.S. Geological Survey data releases: Kaalstad and others (2023) (https://doi.org/10.5066/P97GF4NP) and Martinez and others (2023) (https://doi.org/10.5066/P9C4E2CW).

Declarations

Conflict of Interest The authors declare that they have no conflict of interest.

REFERENCES

Alber M, Swenson EM, Adamowicz SC, Mendelssohn IA. 2008. Salt marsh dieback: an overview of recent events in the US. Estuarine Coastal and Shelf Science 80:1–11.

Allen CD, Macalady AK, Chenchouni H, Bachelet D, McDowell N, Vennetier M, Kitzberger T, Rigling A, Breshears DD, Hogg EH, Gonzalez P, Fensham R, Zhang Z, Castro J, Demidova N, Lim JH, Allard G, Running SW, Semerci A, Cobb N. 2010. A global overview of drought and heat-induced tree mortality reveals emerging climate change risks for forests. Forest Ecology and Management 259:660–684.

Alonso A, Muñoz-Carpena R, E. Kennedy R, Murcia C. 2016. Wetland landscape spatio-temporal degradation dynamics using the new google earth engine cloud-based platform: opportunities for non-specialists in remote sensing. Transactions of the ASABE 59:1331.

Bardou R, Aerni KE, Alemu JB, Armitage AR, Breithaupt JL, Cebrian J, Crimian R, Cummins K, Day RH, Devlin DJ, Doty J, Dunton KH, Enwright NM, Feher LC, Feller IC, Gabler CA, Gibbs SL, Hester MW, Hughes AR, Kang C, Lamont MM, Liu KB, Martinez M, Matheny AM, McClenachan GM, McKee KL, Mendelssohn IA, Michot TC, Miller CJ, Moon JA, Moyer RP, O'Connor R, O'Donnell K, Osland MJ, Pitchford JL, Preheim L, Quirk T, Scheffel WA, Scyphers S, Shepard C, Snyder CM, Sparks E, Swanson KM, Swinea S, Thorne K, Truskey S, Vervaeke WC, Weaver CA, Willis J, Yao Q. 2022. Mangrove distribution in the southeastern United States in 2021: U.S. Geological Survey data release. https://doi.org/10.5066/P9Y2T0K4

Bardou R, Osland MJ, Scyphers S, Shepard C, Aerni KE, Alemu I JB, Crimian R, Day RH, Enwright NM, Feher LC, Gibbs SL, O'Donnell K, Swinea SH, Thorne K, Truskey S, Armitage AR, Baker R, Breithaupt JL, Cavanaugh KC, Cebrian J, Cummins K, Devlin DJ, Doty J, Ellis WL, Feller IC, Gabler CA, Kang Y, Kaplan DA, Kennedy JP, Krauss KW, Lamont MM, Liu K, Martinez M, Matheny AM, McClenachan GM, McKee KL, Mendelssohn IA, Michot TC, Miller CJ, Moon JA, Moyer RP, Nelson J, O'Connor R, Pahl JW, Pitchford JL, Proffitt CE, Quirk T, Radabaugh KR, Scheffel WA, Smee DL, Snyder CM, Sparks E, Swanson KM, Vervaeke WC, Weaver CA, Willis J, Yando ES, Yao Q, Hughes AR. 2023. Rapidly changing range limits in a warming world: critical data limitations and knowledge gaps for advancing understanding of mangrove range dynamics in the southeastern USA. Estuaries and Coasts 46:1123–1140.

Boucek RE, Gaiser EE, Liu H, Rehage JS. 2016. A review of subtropical community resistance and resilience to extreme cold spells. Ecosphere 7:e01455.

Cavanaugh KC, Kellner JR, Forde AJ, Gruner DS, Parker JD, Rodriguez W, Feller IC. 2014. Poleward expansion of mangroves is a threshold response to decreased frequency of extreme cold events. Proceedings of the National Academy of Sciences 111:723–727.

Cavanaugh KC, Osland MJ, Bardou R, Hinojosa-Arango G, López-Vivas JM, Parker JD, Rovai AS. 2018. Sensitivity of mangrove range limits to climate variability. Global Ecology and Biogeography 27:925–935.

Cavanaugh KC, Dangremond EM, Doughty CL, Williams AP, Parker JD, Hayes MA, Rodriguez W, Feller IC. 2019. Climate-driven regime shifts in a mangrove–salt marsh ecotone over the past 250 years. Proceedings of the National Academy of Sciences 116:21602–21608.

Chen L, Wang W, Li QQ, Zhang Y, Yang S, Osland MJ, Huang J, Peng C. 2017. Mangrove species' responses to winter air temperature extremes in China. Ecosphere 8:e01865.

Coldren GA, Proffitt CE. 2017. Mangrove seedling freeze tolerance depends on salt marsh presence, species, salinity, and age. Hydrobiologia 803:159–171.

Cook-Patton SC, Lehmann M, Parker JD. 2015. Convergence of three mangrove species towards freeze-tolerant phenotypes at an expanding range edge. Functional Ecology 29:1332–1340.

Daly C, Helmer EH, Quiñones M. 2003. Mapping the climate of Puerto Rico, Vieques and Culebra. International Journal of Climatology 23:1359–1381.

Daly C, Halbleib M, Smith JI, Gibson WP, Doggett MK, Taylor GH, Curtis J, Pasteris PP. 2008. Physiographically sensitive mapping of climatological temperature and precipitation across the conterminous United States. International Journal of Climatology 28:2031–2064.

Daly C, Widrlechner MP, Halbleib MD, Smith JI, Gibson WP. 2012. Development of a new USDA plant hardiness zone map for the United States. Journal of Applied Meteorology and Climatology 51:242–264.

Day RH, Twilley R, Michot T, From AS. 2020. Geographic distribution of black mangrove (*Avicennia germinans*) in coastal Louisiana in 2009: U.S. Geological Survey data release. https://doi.org/10.5066/P9RC8EIE

Devaney JL, Lehmann M, Feller IC, Parker JD. 2017. Mangrove microclimates alter seedling dynamics at the range edge. Ecology 98:2513–2520.

Duke N, Ball M, Ellison J. 1998. Factors influencing biodiversity and distributional gradients in mangroves. Global Ecology & Biogeography Letters 7:27–47.

Enwright NM, Soo Hoo WM, Dugas JL, Conzelmann CP, Laurenzano C, Lee DM, Mouton K, Stelly SJ. 2020. Louisiana Barrier Island Comprehensive Monitoring Program: Mapping habitats in beach, dune, and intertidal environments along the Louisiana Gulf of Mexico shoreline, 2008 and 2015–16. Reston, VA: U.S. Geological Survey Open-File Report 2020–1030, 57 p. https://doi.org/10.3133/ofr20201030

Feller IC, Berger U, Chapman SK, Dangremond EM, Dix NG, Langley JA, Lovelock CE, Osborne TZ, Shor AC, Simpson LT. 2023. Nitrogen addition increases freeze resistance in black mangrove *(Avicennia germinans)* shrubs in a temperate-tropical ecotone. Ecosystems 26:800–814. https://doi.org/10.1007/s10021-022-00796-z

Finkbeiner M, Simons JD, Robinson C, Wood J, Summers A, Lopez C. 2009. Atlas of shallow-water benthic habitats of coastal Texas: Espiritu Santo Bay to Lower Laguna Madre, 2004 and 2007. Charleston, SC: NOAA Coastal Services Center.

Frazier AE, Hemingway BL. 2021. A technical review of planet smallsat data: practical considerations for processing and using PlanetScope imagery. Remote Sensing 13:3930.

Frazier AE, Wang L. 2013. Modeling landscape structure response across a gradient of land cover intensity. Landscape Ecology 28:233–246.

Gabler CA, Osland MJ, Grace JB, Stagg CL, Day RH, Hartley SB, Enwright NM, From AS, McCoy ML, McLeod JL. 2017. Macroclimatic change expected to transform coastal wetland ecosystems this century. Nature Climate Change 7:142–147.

Gao B. 1996. NDWI—A normalized difference water index for remote sensing of vegetation liquid water from space. Remote Sensing of Environment 58:257–266.

Gitelson AA, Kaufman YJ, Stark R, Rundquist D. 2002. Novel algorithms for remote estimation of vegetation fraction. Remote Sensing of Environment 80:76–87.

Google Earth Engine. 2022. Google Earth Engine.

Hesterberg SG, Jackson K, Bell SS. 2022. Climate drives coupled regime shifts across subtropical estuarine ecosystems. Proceedings of the National Academy of Sciences 119:e2121654119.

Hoffman SE, Devlin DJ, Proffitt CE. 2022. Maternal nutrient history enhances black mangrove (*Avicennia germinans*) seedling growth after propagules experience a hard freeze. Estuaries and Coasts 45:2534–2542.

Hufkens K, Ceulemans R, Scheunders P. 2008. Estimating the ecotone width in patchy ecotones using a sigmoid wave approach. Ecological Informatics 3:97–104.

IPCC. 2021. Summary for policymakers. In: Masson-Delmotte V, Zhai P, Pirani A, Connors SL, Péan C, Berger S, Caud N, Chen Y, Goldfarb L, Gomis MI, Huang M, Leitzell K, Lonnoy E, Matthews JBR, Maycock TK, Waterfield T, Yelekçi O, Yu R, Zhou B, editors. Climate Change 2021: The Physical Science Basis. Contribution of Working Group I to the Sixth Assessment Report of the Intergovernmental Panel on Climate Change. Cambridge: Cambridge University Press. pp 3–32. https://doi.org/10.1017/9781009157896.001

Jentsch A, Kreyling J, Beierkuhnlein C. 2007. A new generation of climate-change experiments: events, not trends. Frontiers in Ecology and the Environment 5:365–374.

Kaalstad S, Devlin DJ, Proffitt CE, Osland MJ, Swanson KM, Kaplan DA, Day RH, Feher LC, Reever NGF, Dunton KH, Stetter AP, Fierro-Cabo A, From AS, Cebrian J, Miller CJ, Cummins KL, Armitage AR, Sanspree CR, Flores EA, Hughes R, Zamora-Tovar C, Snyder CM, Thompson JE, Anderson GH. 2023. 2021 Gulf of Mexico Mangrove Freeze Damage Data: U.S. Geological Survey data release, https://doi.org/10.5066/P97GF4NP.

Kennedy JP, Preziosi RF, Rowntree JK, Feller IC. 2020. Is the central-marginal hypothesis a general rule? Evidence from three distributions of an expanding mangrove species, *Avicennia germinans* (L.) L. Molecular Ecology 29:704–719.

Kennedy JP, Johnson GN, Preziosi RF, Rowntree JK. 2022. Genetically based adaptive trait shifts at an expanding mangrove range margin. Hydrobiologia 849:1777–1794.

Lagomasino D, Fatoyinbo T, Castañeda-Moya E, Cook BD, Montesano PM, Neigh CSR, Corp LA, Ott LE, Chavez S, Morton DC. 2021. Storm surge and ponding explain mangrove dieback in southwest Florida following Hurricane Irma. Nature Communications 12:4003.

Langston AK, Kaplan DA. 2020. Modelling the effects of climate, predation, and dispersal on the poleward range expansion of black mangrove (*Avicennia germinans*). Ecological Modelling 434:109245.

Lonard RI, Judd FW. 1991. Comparison of the effects of the severe freezes of 1983 and 1989 on native woody plants in the lower Rio Grande Valley. Texas. the Southwestern Naturalist 36:213.

Lovelock CE, Krauss KW, Osland MJ, Reef R, Ball MC. 2016. The physiology of mangrove trees with changing climate. In: Goldstein G, Santiago LS, editors. Tropical Tree Physiology: Adaptations and Responses in a Changing Environment. Tree Physiology. Cham: Springer International Publishing. pp 149–79.

Lugo AE, Patterson-Zuca C. 1977. The impact of low temperature stress on mangrove structure and growth. Tropical Ecology. 18:149–161.

Macy A, Osland MJ, Cherry JA, Cebrian J. 2021. Effects of chronic and acute stressors on transplanted black mangrove (*Avicennia germinans*) seedlings along an eroding Louisiana shoreline. Restoration Ecology 29:e13373.

Madrid EN, Armitage AR, López-Portillo J. 2014. *Avicennia germinans* (black mangrove) vessel architecture is linked to chilling and salinity tolerance in the Gulf of Mexico. Frontiers in Plant Science 5:503.

Martin JH, McEachron LW. 1996. Historical annotated review of winter kills of marine organisms in Texas bays. Austin, TX: Texas Parks and Wildlife - Coastal Fisheries Division

Martinez M, Osland MJ, Grace JB, Enwright NM, Stagg CL, Kaalstad S, Anderson G, Armitage AR, Cebrian J, Cummins KL, Day RH, Devlin DJ, Dunton KH, Feher LC, Fierro-Cabo A, Flores EA, From AS, Hughes AR, Kaplan DA, Langston AK, Miller C, Proffitt CE, Reaver NGF, Sanspree CR, Snyder CM, Stetter AP, Swanson KM, Thompson JE, Zamora-Tovar C. 2023. Integrating remote sensing with ground-based observations to quantify the effects of an extreme freeze event on black mangroves (*Avicennia germinans*) at the landscape scale: U.S. Geological Survey data release, https://doi.org/10.5066/P9C4E2CW.

McClenachan G, Witt M, Walters LJ. 2021. Replacement of oyster reefs by mangroves: Unexpected climate-driven ecosystem shifts. Global Change Biology 27:1226–1238.

McKee KL, Vervaeke WC. 2018. Will fluctuations in salt marsh–mangrove dominance alter vulnerability of a subtropical wetland to sea-level rise? Global Change Biology 24:1224–1238.

Narron CR, O'Connell JL, Mishra DR, Cotten DL, Hawman PA, Mao L. 2022. Flooding in Landsat across tidal systems (FLATS): An index for intermittent tidal filtering and frequency detection in salt marsh environments. Ecological Indicators 141:109045.

NOAA. 2022. Global historical climatology network daily. Climate Data Online - National Climatic Data Center.

Office for Coastal Management. 2022. C-CAP Derived 10 meter Land Cover—BETA from 2010–06–15 to 2010–08–15.

Osland MJ, Day RH, Larriviere JC, From AS. 2014. Aboveground allometric models for freeze-affected black mangroves *(Avicennia germinans)*: equations for a climate sensitive mangrove-marsh ecotone. PLOS ONE 9:e99604.

Osland MJ, Day RH, Hall CT, Brumfield MD, Dugas JL, Jones WR. 2017. Mangrove expansion and contraction at a poleward range limit: climate extremes and land-ocean temperature gradients. Ecology 98:125–137.

Osland MJ, Hartmann AM, Day RH, Ross MS, Hall CT, Feher LC, Vervaeke WC. 2019. Microclimate influences mangrove freeze damage: implications for range expansion in response to changing macroclimate. Estuaries and Coasts 42:1084–1096.

Osland MJ, Day RH, Hall CT, Feher LC, Armitage AR, Cebrian J, Dunton KH, Hughes AR, Kaplan DA, Langston AK, Macy A, Weaver CA, Anderson GH, Cummins K, Feller IC, Snyder CM. 2020. Temperature thresholds for black mangrove (*Avicennia germinans*) freeze damage, mortality and recovery in North America: Refining tipping points for range expansion in a warming climate. Journal of Ecology 108:654–665.

Osland MJ, Stevens PW, Lamont MM, Brusca RC, Hart KM, Waddle JH, Langtimm CA, Williams CM, Keim BD, Terando AJ, Reyier EA, Marshall KE, Loik ME, Boucek RE, Lewis AB, Seminoff JA. 2021. Tropicalization of temperate ecosystems in North America: The northward range expansion of tropical organisms in response to warming winter temperatures. Global Change Biology 27:3009–3034.

Osland MJ, Day RH, From AS, McCoy ML, McLeod JL, Kelleway JJ. 2015. Life stage influences the resistance and resilience of black mangrove forests to winter climate extremes. Ecosphere 6:art160.

Osland MJ, Hughes AR, Armitage AR, Scyphers SB, Cebrian J, Swinea SH, Shepard CC, Allen MS, Feher LC, Nelson JA, O'Brien CL, Sanspree CR, Smee DL, Snyder CM, Stetter AP, Stevens PW, Swanson KM, Williams LH, Brush JM, Marchionno J, Bardou R. 2022. The impacts of mangrove range expansion on wetland ecosystem services in the southeastern United States: Current understanding, knowledge gaps, and emerging research needs. Global Change Biology 28:3163–3187.

Pennings SC, Bertness MD. 2001. Salt marsh communities. In: Marine Community Ecology. In M.D. Bertness, S.D. Gaines, M. Hay. Sunderland, Massachusetts. pp 289–316.

Pickens CN, Hester MW. 2011. Temperature tolerance of early life history stages of black mangrove *Avicennia germinans*: implications for range expansion. Estuaries and Coasts 34:824–830.

Purtlebaugh CH, Martin CW, Allen MS. 2020. Poleward expansion of common snook *Centropomus undecimalis* in the northeastern Gulf of Mexico and future research needs. PLOS ONE 15:e0234083.

R Core Team. 2022. R: A language and environment for statistical computing.

Ritz C, Strebig JC. 2016. Analysis of Dose-Response Curves.

Ross MS, Ruiz PL, Sah JP, Hanan EJ. 2009. Chilling damage in a changing climate in coastal landscapes of the subtropical zone: a case study from south Florida. Global Change Biology 15:1817–1832.

Rouse JW, Hass RH, Schell JA, Deering DW. 1974. Monitoring vegetation systems in the Great Plains with ERTS. 3rd Earth Resource Technology Satellite (ERTS) 1:48–62.

Sherrod CL, McMillan C. 1981. Black mangrove, *Avicennia germinans*, in Texas: past and present distribution. Contributions in Marine Science 24:115–131.

Sherrod CL, McMillan C. 1985. The distributional history and ecology of mangrove vegetation along the northern Gulf of Mexico coastal region. Contributions in Marine Science 28:129–140.

Shreve F. 1914. The role of winter temperatures in determining the distribution of plants. American Journal of Botany 1:194–202.

Sippo JZ, Lovelock CE, Santos IR, Sanders CJ, Maher DT. 2018. Mangrove mortality in a changing climate: An overview. Estuarine, Coastal and Shelf Science 215:241–249.

Smith MD. 2011. An ecological perspective on extreme climatic events: a synthetic definition and framework to guide future research. Journal of Ecology 99:656–663.

Snyder CM, Feher LC, Osland MJ, Miller CJ, Hughes AR, Cummins KL. 2022. The distribution and structure of mangroves (*Avicennia germinans* and *Rhizophora mangle*) near a rapidly changing range limit in the northeastern Gulf of Mexico. Estuaries and Coasts 45:181–195.

Stevens PW, Fox SL, Montague CL. 2006. The interplay between mangroves and saltmarshes at the transition between temperate and subtropical climate in Florida. Wetlands Ecology and Management 14:435–444.

Tahsin S, Medeiros SC, Singh A. 2018. Assessing the resilience of coastal wetlands to extreme hydrologic events using vegetation indices: a review. Remote Sensing 10:1390.

Timoney KP, La Roi GH, Dale MRT. 1993. Subarctic forest-tundra vegetation gradients: the sigmoid wave hypothesis. Journal of Vegetation Science 4:387–394.

Tomlinson PB. 2016. The botany of mangroves, 2nd edn. Cambridge: Cambridge University Press.

USGCRP. 2017. Climate Science Special Report: Fourth National Climate Assessment, Volume I. U.S. Global Change Research Program, Washington, DC

USGCRP. 2018. Fourth National Climate Assessment: Impacts, Risks, and Adaptation in the United States: Fourth National Climate Assessment, Volume II. U.S. Global Change Research Program, Washington, DC

Walters LJ, McClenachan G. 2021. Commentary on Osland et al.: Tropicalization of temperate ecosystems in North America: The northward range expansion of tropical organisms in response to warming winter temperatures. Global Change Biology 27:3006–3008.

Wang L, Jia M, Yin D, Tian J. 2019. A review of remote sensing for mangrove forests: 1956–2018. Remote Sensing of Environment 231:111223.

Weaver CA, Armitage AR. 2018. Nutrient enrichment shifts mangrove height distribution: Implications for coastal woody encroachment. PLOS ONE 13:e0193617.

Wilson JB, Agnew ADQ. 1992. Positive-feedback switches in plant communities. In: Advances in Ecological Research. Vol. 23. Academic Press. pp 263–336.

Woodroffe CD, Grindrod J. 1991. Mangrove biogeography: the role of quaternary environmental and sea-level change. Journal of Biogeography 18:479–492.

Yando ES, Osland MJ, Willis JM, Day RH, Krauss KW, Hester MW. 2016. Salt marsh-mangrove ecotones: using structural gradients to investigate the effects of woody plant encroachment on plant–soil interactions and ecosystem carbon pools. Journal of Ecology 104:1020–1031.

Zhang K, Thapa B, Ross M, Gann D. 2016. Remote sensing of seasonal changes and disturbances in mangrove forest: a case study from South Florida. Ecosphere 7:e01366.